

**OPTOGENETIC SUPPRESSION OF MEDIAL  
PREFRONTAL CORTEX- AND DORSAL HIPPOCAMPUS-  
NUCLEUS REUNIENS PATHWAYS  
IMPAIRS SPATIAL WORKING MEMORY**

by

Jackson Mace

A thesis submitted to the Faculty of the University of Delaware in partial fulfillment of the requirements for the degree of Neuroscience with Distinction

Spring 2020

© 2020 Jackson Mace  
All Rights Reserved

**OPTOGENETIC SUPPRESSION OF MEDIAL  
PREFRONTAL CORTEX- AND DORSAL HIPPOCAMPUS-  
NUCLEUS REUNIENS PATHWAYS  
IMPAIRS SPATIAL WORKING MEMORY**

by

Jackson Mace

Approved: \_\_\_\_\_  
Amy Griffin, Ph.D.  
Professor in charge of thesis on behalf of the Advisory Committee

Approved: \_\_\_\_\_  
Jeffrey Rosen, Ph.D.  
Committee member from the Department of Department Name

Approved: \_\_\_\_\_  
Jaclyn Schwarz, Ph.D.  
Committee member from the Board of Senior Thesis Readers

Approved: \_\_\_\_\_  
Michael Chajes, Ph.D.  
Chair of the University Committee on Student and Faculty Honors

## ACKNOWLEDGMENTS

I want to first thank my family for encouraging me and checking up on me every now and then to make sure that I still am going to classes on Zoom. Without them, I would have never made it to the University of Delaware and pursued my fresh interests. I would like to thank the following lab members who have helped me collect behavioral data over the past 3 years and have mentored me when I first joined the laboratory as a freshman in college: Natalie Looney, Morgan Gaylord, and Bernardus Willems. Similarly, I want to thank Henry Hallock, Brett Emanuel, and Andrew Garcia for starting this project before I joined the lab. I would also like to thank Zachary Gemzik for helping me with many of this study's procedures, such as virally injecting rats prior to testing and preparing rat brains for postmortem histology. Additionally, I want to thank John Stout for helping me compile and statistically analyze all of this study's data. I also want to thank my second and third senior thesis readers, Dr. Jeffrey Rosen and Dr. Jaclyn Schwarz, for providing me with useful comments throughout the thesis process while offering me constant advice about choosing my future graduate program. Finally, I want to thank my lab's principal investigator that I have worked under for all 4 years of college, Dr. Amy Griffin – without her, I would have never ended up discovering my passion for neuroscience research (through projects such as this one) and chasing it to the fullest extent (getting accepted to my top-ranked neuroscience Ph.D. program for the coming Fall).

## TABLE OF CONTENTS

LIST OF FIGURES .....	v
ABSTRACT .....	vi
1 Introduction .....	1
2 Methods .....	5
2.1 Subjects.....	5
2.2 Behavioral apparatus and DNMP task paradigm .....	5
2.3 Training protocol.....	6
2.4 Surgical procedure.....	7
2.5 DNMP testing and optogenetics .....	9
2.6 Histology .....	10
2.7 Statistical analysis .....	11
3 Results .....	13
3.1 Fiber placement and viral expression .....	13
3.2 Histology reporting.....	15
3.3 Behavioral reporting.....	16
3.4 dHPC-Re input is necessary for encoding spatial memories on DNMP task.....	17
3.5 mPFC-Re input is necessary for encoding and retrieving spatial memories on DNMP task .....	19
4 Discussion.....	23
4.1 Significance .....	23
4.2 Functional role of anatomical connectivity across the mPFC-Re-HPC circuit.....	23
4.3 Re is implicated in orchestrating mPFC-HPC interactions during select SWM components .....	25
4.4 Conclusions .....	28
REFERENCES .....	29

**LIST OF FIGURES**

Figure 1: Exemplary histology and viral spread report.....14

Figure 2: mPFC and dHPC input to Re during different DNMP task phases.....21

## **ABSTRACT**

The medial prefrontal cortex (mPFC), dorsal hippocampus (dHPC), and nucleus reuniens (Re) of the midline thalamus have been demonstrated to be necessary for spatial working memory (SWM). Previous studies have implicated the mPFC-HPC interactions as crucial for supporting accurate SWM performance. Past work has also revealed the Re as a key component for mediating these mPFC-dHPC interactions during a SWM task. However, little work has described how this circuit contributes to the three core components of SWM: memory encoding, memory maintenance, and memory retrieval. With previous evidence that began to understand how the outputs from the Re contribute to memory encoding as opposed to memory maintenance and retrieval, this new study examines the inputs from the mPFC and dHPC to the Re. We used optogenetic suppression techniques to selectively perturb pathways from the mPFC and dHPC to the Re. We also utilized a delayed non-match to position task to parse apart SWM into its three core components. We demonstrated that disrupting synaptic projections from the dHPC to the Re in rats disrupted their ability to encode memories. We determined that suppressing synaptic projections from the mPFC to the Re in rats disturbed their ability to encode and retrieve memories. These findings highlight the Re as a vital component for coordinating mPFC-dHPC interactions during memory encoding. The results also show that Re-mPFC interactions are critical

for memory retrieval. Altogether, this study will establish a better understanding of the neural circuitry underlying SWM, enabling doctors to better address working memory deficits in humans that are associated with many neurological disorders.

## **Chapter 1**

### **Introduction**

Spatial working memory (SWM) is defined as the ability to store and process spatial information during goal-driven navigation. Several studies have shown that the medial prefrontal cortex (mPFC) and hippocampus (HPC) are important for the acquisition and performance of SWM in rodents (Aggleton et al., 1986; Lee and Kesner, 2003; Wang and Cai, 2006; Churchwell and Kesner, 2011). In a similar vein, various inactivation studies have detailed either the HPC or mPFC as independent structures that can support SWM processes in rats if the temporal gap between when the animal encodes and retrieves a spatial memory remains short (Lee and Kesner, 2003; Churchwell and Kesner, 2011). When considering these two regions during a prolonged memory maintenance period, both the mPFC and HPC are necessary for SWM (Wang and Cai, 2006; Churchwell and Kesner, 2011).

While it has been shown that the dorsal HPC (dHPC) is essential for accurate performance on SWM tasks, the distinct synaptic projections from the HPC to the mPFC mostly originate in the intermediate and ventral regions of the HPC as opposed to the dorsal regions (Jay and Witter 1991; Hoover and Vertes 2007; Czerniawski et al., 2009). Additionally, minimal mPFC projections to the HPC have been shown to exist (Rajaseethupathy et al., 2015). Most data show mPFC-HPC interactions occur via

indirect synaptic pathways (Eichenbaum, 2017; Dolleman-van der Weel et al., 2019), possibly mediated by relay nuclei.

The nucleus reuniens (Re) of the midline thalamus has been described as another crucial contributor to SWM (Griffin, 2015; Dolleman-van der Weel et al., 2019). The Re is not only an important relay center along with other thalamic nuclei, but it also has been implicated as a fundamental region that supports higher-order cortico-thalamo-cortical circuitry (Vertes et al., 2006; Vertes et al., 2007; Dolleman-van der Weel et al., 2019). One example of this higher order circuitry that we will examine in our study is the communication that exists between the mPFC and HPC, which is supported by the Re. The Re projects to both the mPFC and HPC (Herkenham, 1978; Vertes et al., 2006). It also receives input from the mPFC, HPC, and many other subcortical regions (McKenna and Vertes, 2004). Interestingly, some individual Re neurons project via collaterals to both the mPFC and HPC (Hoover and Vertes, 2012). Moreover, some mPFC projections to the Re synapse on HPC-projecting neurons (Vertes et al., 2007), which reveals a possible intermediate area where inter-regional interactions between the mPFC and HPC are occurring. Altogether, while it has been shown that the mPFC and HPC interactions with each other and with the Re are important for SWM tasks, the exact contributions to memory functions that these interactions can be attributed with remain unknown.

In support of the Re acting as a region that mediates the communication between the mPFC and HPC, past studies have shown that pharmacologically inactivating the Re and rhomboid nuclei (Rh) of the ventral midline thalamus in rats

impairs their performance on a SWM task (Layfield et al., 2015; Hallock et al., 2016; Viena et al., 2018). When simultaneously inactivating both the Re and Rh, Hallock et al., (2016) elucidated that HPC-mPFC theta coherence (4-12 Hz) decreased. In the same study, low theta coherence was correlated with low performance accuracy on the SWM task, while high theta coherence was correlated with accurate performance on the SWM task. Hallock et al., (2016) also demonstrated that pharmacological inactivation of the Re and Rh reduced mPFC single-unit entrainment to HPC theta and impaired HPC theta-mPFC gamma cross-frequency coupling. Consistent with these findings, Ito et al., (2015) showed that perturbing Re activity led to impaired HPC trajectory-dependent firing on a SWM task. As a result, these details suggest that the mPFC regulates trajectory-dependent firing activity that exists in the HPC via the Re.

While it is likely that the Re is vital for mediating mPFC-HPC interactions, only recently has our lab revealed how Re output contributes to memory when examining the various components of SWM: memory encoding, memory maintenance, and memory retrieval. Maisson et al., (2018) showed that Re suppression during memory encoding, but not during memory maintenance or retrieval, decreased a rat's choice accuracy on a delayed non-match to position (DNMP) task. Now that output projections from the Re have been attributed to a distinct role in supporting SWM, it is most logical to examine how the main input projections to the Re contribute to specific components of SWM.

Because the Re is important for supporting mPFC-HPC interactions during SWM tasks and is required for encoding spatial information on a DNMP paradigm, we

postulated that the Re coordinates mPFC-HPC interactions during memory encoding. Specifically, we hypothesized that projections from the mPFC and dHPC to the Re during the encoding phase of a SWM task are needed for accurate SWM performance. In order to explore the exact contributions of the mPFC-Re and the dHPC-Re synaptic projections during a SWM task, this current study used optogenetic suppression techniques to selectively inhibit each of the two individual pathways at temporally precise points along the DNMP task. These data elucidate whether mPFC-Re and dHPC-Re pathways contribute to SWM, specifically if the pathways are necessary for memory encoding, memory maintenance, and/or memory retrieval. From these findings, we will have a better understanding of the neural circuitry underlying SWM, which will allow scientists and doctors to better address working memory deficits in humans that are often associated with neuropsychiatric disorders such as schizophrenia and ADHD.

## **Chapter 2**

### **Methods**

#### **2.1 Subjects**

Long Evans hooded rats from ENVIGO (Somerset, New Jersey) were used throughout this study. These experiments only utilized male rats that were older than 90 days of age. Prior to starting an experiment, each rat was confirmed to weigh more than 350 grams. Throughout the training and testing periods, all rats were kept on a food-restricted diet, limiting them to 4-5 standard rat chow pellets per day to keep them at about 90% of their pre-experimentation weight. All rats were housed in individual cages within a colony room that was controlled for temperature and humidity. This room also maintained a 12-hour light/dark cycle to mimic a real environment for the rats. All rats were trained and tested during the active 12-hour light cycle. Each procedure utilizing a rat was approved and monitored by the University of Delaware's Institutional Animal Care and Use Committee.

#### **2.2 Behavioral apparatus and DNMP task paradigm**

The behavioral training and testing apparatus used in this study was the same that was used in Maisson et al., (2018). A wooden T-maze sat in the center of a dimly lit small, square-shaped room. The maze had white floors and sides. Each side of the room was covered by a black curtain. The black curtains displayed unique visual cues

to provide spatial context for the rat when performing the SWM task on the T-maze. A rectangular-shaped start box sat at the beginning of the maze stem, or at the beginning of the “T.” Return arms that led back to the start box were attached to each of the two reward zones. Both reward zones held chocolate sprinkles. Now considering the delayed non-match to position (DNMP) task, the rat first began in the start box and was kept there with a wooden stopper. The stopper blockade was lifted up after 20 seconds and the rat ran down the center of the “T,” until approaching the decision point. For the first sample traversal, or memory encoding period, the rat was forced to go either left or right at the decision point of the maze. It retrieved the reward on the side it was forced toward and went back to the start box for 20 seconds to experience the delay period, or the memory maintenance phase. The rat then ran down the center of the “T” once again, and had the opportunity to choose to go toward the same side it was just forced to (and not receive a reward since it had been depleted), or attend the novel side that it did not previously go to (and receive a reward). This final part of the task was considered the choice traversal, or the memory retrieval period. See Figure 2A for further explanation of the task.

### **2.3 Training protocol**

The behavioral training used in this study was the same that was used in Maisson et al., (2018). Each rat was handled for one week before any behavioral training began. After this, rats underwent “goal-box” training, where they were exposed to the reward zones and began consuming the chocolate sprinkles in less than

90 seconds per exposure period. This training finished after the rats consumed the sprinkles within the time constraint for two consecutive days. From here, the rats began “forced-run” training, where they learned to move along the T-maze. Once the rats demonstrated that they were capable of running the course of the maze without stopping and consume the reward without turning around for at least two days in a row, they received the viral injection surgery on either the mPFC or dHPC site. After the surgery, each rat had a 5-day recovery period before advancing to DNMP task training. Rats were trained on the DNMP task for 6 days/week until they reliably performed it with  $\geq 80\%$  choice accuracy for two consecutive days. After DNMP task training criterion was met, rats underwent the fiber implant surgery on the Re site, recovered for 5 days, and were quickly retrained on the DNMP task. After re-meeting criterion, the rats’ fiber was connected to the optogenetics cable so that they could become acquainted with running the DNMP task while properly tethered. This pre-DNMP testing, with the tether attached, went on for 1 day. Afterward, DNMP testing began.

## **2.4 Surgical procedure**

The two survival surgeries that each rat underwent followed the same guidelines as outlined in Maisson et al., (2018). Each rat was randomly put into one of the following categories: the control virus (AAV-5-CAG-tdTomato, Boyden Lab stock, UNC Vector Core, titer  $<10^{12}$   $\mu\text{g/ml}$ ) and the neural suppressor virus (AAV5-CAG-ArchT-tdTomato, Boyden Lab stock, UNC Vector Core, titer  $<10^{12}$   $\mu\text{g/ml}$ ). In

each category, two groups were created. One group in the control virus category received its viral injections into the mPFC. Another group in the control virus category received its viral injections into the dHPC. One group in the neural suppressor virus category received its viral injections into the mPFC. Another group in the neural suppressor virus category received its viral injections into the dHPC. The viral infusion surgery took place between pre-training and DNMP task training. This allowed the rat to be evaluated on whether it could run along the maze before undergoing surgery. After the rat had its viral injection surgery, a 5-week viral expression (dHPC-Re and mPFC-Re pathways) period was allotted. The dHPC virus surgery comprised of two injections to each hemisphere of the brain. In each hemisphere, the first two craniotomies were made at 5.3 mm posterior and 1.2 mm lateral to bregma. The virus injection occurred at a depth of 3.2 mm ventral to the dura. The second craniotomies in each hemisphere were made at 5 mm posterior and 3.2 mm lateral to bregma. The virus injection occurred at a depth of 2.5 mm ventral to the dura. The mPFC surgery also had two injections per brain hemisphere. A 1 mm craniotomy was directed in the midline of the skull at 3.2 mm anterior to bregma. At 0.5 mm lateral to the midline, the injections were delivered at depths of 4.6 mm and 2.7 mm ventral to dura.

The second surgery, the fiber implantation dorsal to the Re, took place once the rats reached criterion on the DNMP training task. The new craniotomy for this fiber implantation surgery was made 2.3 mm posterior and 2 mm lateral to bregma. The fiber was implanted at a depth of 7 mm ventral to dura.

## 2.5 DNMP testing and optogenetics

After the 5-day recovery period following the fiber implant surgery, rats were retrained on the DNMP task until performing at a minimum of 80% accuracy for 2 consecutive days. After criterion was met, the rat was tethered in to the optogenetics cable for 1 day to mimic DNMP testing conditions. Following this, three days of DNMP testing took place. Each day was dedicated to optogenetic suppression of either the mPFC-Re or dHPC-Re pathway during a different phase of the task (memory encoding, memory maintenance, memory retrieval) as denoted in Figure 2A. Optogenetic suppression during the memory encoding phase meant that the light was on during the sample traversal. Optogenetic suppression during the memory maintenance phase meant that the light was on during the delay period. Optogenetic suppression during the memory retrieval phase meant that the light was on during the choice traversal. Optogenetic-induced terminal suppression was performed using a 10mW 525 nm light delivered through a fiber optic patch cable and an implanted optical fiber stub (core diameter: 200  $\mu\text{m}$ ; numerical aperture: 0.66). Archaelhodopsin (or ArchT) expression was used for the optogenetic methodology carried out in this study. The ArchT protein is a light-sensitive proton pump that acts as an inhibitory ion channel, when struck by a certain range of light wavelengths, by driving protons against their concentration gradient, outside of the neuron. Positively charged hydrogen atoms leaving the neuron induces a hyperpolarization response. We expressed this channel in the mPFC-Re or dHPC-Re pathways of the rats through the viral surgeries to inhibit the pathways on command via light stimulation. Aside from

the between-group control animals that did not receive the ArchT neural suppressor viral injection, each of the three testing days included a within-group control where the rat would run half of the trials without any active light. The no-light trials were compared to the light-on trials within a single day's session (see Statistical Analysis section of Methods chapter). Thus, each testing session composed of four, six-trial blocks, with optical stimulation occurring in the second and fourth block. Position tracking and automated light activation were attained by using the PlexBright Optogenetic Simulation System (Plexon, Inc., Dallas, TX).

## **2.6 Histology**

One day after DNMP testing was complete, the rats were anesthetized with isoflurane and administered an excessive amount of sodium pentobarbital (Euthasol, 0.5 mL). Next, they were transcardially perfused with 200 mL of 1x Tris-buffered saline (TBS, pH 7.2 – 7.4), immediately followed by 200 mL of 4% paraformaldehyde (PFA 7.2 – 7.4). Each brain was submersion-fixed in 4% PFA for 24 hours, followed by cryoprotection in a 30% sucrose solution. Once the brain sank into this solution, it was sectioned at a thickness of 40  $\mu\text{m}$  at a temperature of  $-20^{\circ}\text{C}$  and mounted to glass microscope slides. The slides were washed with 1x TBS and immersed in a Prolong Diamond with DAPI stain. From there, the slides were sealed with a glass coverslip. Injection sites were imaged to assess whether viral expression to the Re from either the mPFC or the dHPC occurred. Fiber sites were also imaged to confirm that fiber implantations were accurately placed. The Zeiss 880 confocal microscope with a C-

Apochromat 10x/0.45W lens was used for imaging purposes throughout this study. Images were compared to The Rat Brain Atlas (Paxinos & Watson, 2005) to measure the center and the spread of the virus's expression.

## **2.7 Statistical analysis**

To assess the specific task-phase contributions of the mPFC and dHPC projections to the Re, the correct trials in a testing session were compared to the total amount of trials in that session. While we originally ran 2 by 2 mixed-design ANOVA tests, we only noted trending light-by-group interactions due to the limited number of rats that we used in this study along with the small range of possible performance variations on the DNMP task when comparing subjects. Very few of our rats consistently perform below chance and between 90-100% accuracy on the DNMP paradigm. Mirroring this, almost all of our study's rats performed between 65-80% accuracy on the task irrespective of manipulations. Therefore, we considered this information early on and decided that for each of the light condition-specific testing sessions (sample traversal, delay period, and choice traversal), a paired samples t-test would be used to analyze the choice accuracy data. These planned comparisons were utilized to measure the differences in performance accuracy when the light was on versus when the light was off in the tdTomato control animals and ArchT experimental animals. However, we did report the ANOVA statistics regarding the overall light effects that were occasionally noted between ArchT+ and ArchT- groups. During the three days of DNMP task testing, if a rat's fiber implantation fell out, the

rat was removed from the study. Similarly, if the rat's choice accuracy was at or below 50% during the first light-off control trial block, or if its choice accuracy was at or below 67% during the first light-off control trials with a total session average of less than or equal to 67% choice accuracy on all light-off trials, that rat's session data was excluded from the final analysis. Green & Stanton (1989) demonstrated this criterion by showing that rats spontaneously alternate at 67% accuracy. This study determined statistical significance values by utilizing a standard alpha level of  $<0.05$ . MATLAB and R were used for all statistical computations.

## Chapter 3

### Results

#### 3.1 Fiber placement and viral expression

ArchT is activated at a peak wavelength of 566 nm, and therefore only green and yellow light can be used for expressing ArchT (Yizhar et al., 2011). Light only penetrates to about 2 mm through a saline solution, with a reduction of less than 10% of the light's original power after reaching a projection distance of 0.5 mm (Smith & Smith, 2014). Thus, in our study, we attempted to confirm that the rats' expression of fluorescence in either the mPFC-Re (Figure 1A-B) or the dHPC-Re (Figure 1C-D) pathways projected beneath the fiber tip end closest to the dorsal Re. In all the rats, the tip of the optical fiber was located at a mean distance of 0.47 mm (SD = 0.33) from the top of the Re. The fiber that was implanted into the rats emitted a right circular cone of green light at a height of 1.5 mm, which embodied a volume of  $3.53 \text{ mm}^3$  ( $V = \pi r^2(h/3)$ ). The implanted fiber also had a numerical aperture of 0.66 NA. Altogether, all rats used in the statistical analysis of this study, other than 6 control rats that have not been verified through histology reports yet because of the COVID-19 pandemic, were confirmed to have their Re in the range of optical stimulation.

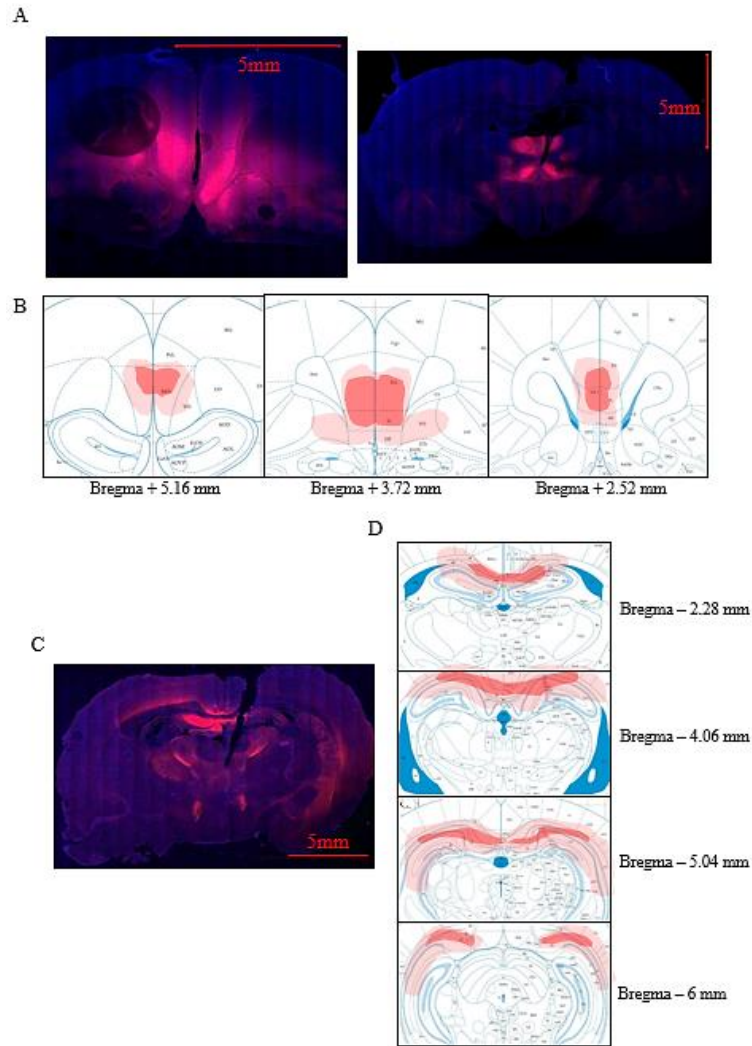


Figure 1: Exemplary histology and viral spread

This figure illustrates the histological confirmation procedure of the implanted fiber tips (black dots) as well as representative images of the viral spread and expression (red shading). A.) A representative image of tdTomato fluorescent staining in the mPFC region (left image) and its projections to the Re that appear as further staining beneath the negative space caused by the implanted fiber (right image). B.) Pictures extracted from The Rat Brain Atlas (Paxinos & Watson, 2005) from the most

anterior to the most posterior (left image to right image) that cover the AP extent of the mPFC to show the most (lighter red shade) to the least (darker red shade) viral spread at the defined coordinates. C.) A representative image of tdTomato fluorescent staining in the dHPC and its projections to the Re that appear as further staining beneath the diagonally oriented negative space caused by the implanted fiber. D.) Similar to B, pictures extracted from The Rat Brain Atlas (Paxinos & Watson, 2005) that cover the AP extent of the dHPC with the approximated viral spread at the distinct coordinate.

### **3.2 Histology reporting**

Post-mortem analyses were conducted on 16 total rats: 3 mPFC-tdTomato injection rats, 3 dHPC-tdTomato injection rats, 5 dHPC-ArchT injection rats, and 5 mPFC-ArchT injection rats. While 22 rats were utilized in this study, due to the unforeseeable nature of all research labs shutting down across the country due to the COVID-19 pandemic, 3 mPFC-tdTomato control rats and 3 dHPC-tdTomato control rats have not been verified via postmortem histological reports yet. Viral injections into the mPFC were placed at bregma + 3.2 mm AP, at midline  $\pm$  0.5 mm ML, and dura - 4.6 mm and - 2.7 mm DV. Viral injections into the dHPC were placed at bregma - 5.3 mm and bregma - 5.8 mm AP, at midline  $\pm$  1.2 mm and  $\pm$  3.2mm ML, and dura + 3.2 mm and - 2.5 mm DV. Along their AP extent, the prelimbic cortex/infralimbic prefrontal cortex expand to about 2.64 mm, the Re about 2.4 mm, and the HPC approximately 4.68 mm (Paxinos & Watson, 2005). Thus, images of

coronal sections were retrieved between  $\pm 3$  mm of the most anterior and posterior injection coordinates for either site (Figure 1B/D) in order to validate whether the AP spread of viral expression penetrated each brain region of interest.

The ML and DV viral spreads were taken in accordance to the approximated center of the AP spread. Both mPFC injections (mPFC-tdTomato control virus and mPFC-ArchT neural suppressor virus) had an average ML viral spread of 1.39 mm (SD = 0.51) in either direction from the midline and an average DV spread of 3.07 mm (SD = 0.81). Both dHPC injections (dHPC-tdTomato control virus and dHPC-ArchT neural suppressor virus) had an average ML viral spread of 3.29 mm (SD = 1.36) in all directions from the midline and an average DV spread of 0.9 mm (SD = 0.56).

### **3.3 Behavioral reporting**

Behavioral analyses were conducted on the same 16 rats that we performed histology analyses on as mentioned in the previous Histology reporting section of the Methods chapter, along with the 6 control rats that have not been confirmed through histology reports yet. Thus, a total of 22 rats were utilized for behavioral analyses. Choice accuracy did not significantly vary between the mPFC-tdTomato and the dHPC-tdTomato control groups. Due to the removal of sessions because a rat did not stay at behavioral criteria during the testing period (see Statistical analysis section of Methods chapter) or the rat experienced a fiber implant breakage, some behavioral data were not included in the final statistical analysis. In the mPFC-tdTomato control group, 5/6 rats completed the sample traversal session, 5/6 rats completed the delay

period session, and 4/6 rats completed the choice traversal session. In the dHPC-tdTomato sub-control group, all 6 rats completed the sample traversal session, 5/6 rats completed the delay period session, and 4/6 rats completed the choice traversal session. In the mPFC-ArchT neural suppressor group, 4/5 rats completed the sample traversal session, 4/5 rats completed the delay period session, and all 5 rats completed the choice traversal session. In the dHPC-ArchT neural suppressor group, all 5 rats completed the sample traversal session, 4/5 rats completed the delay period session, and all 5 rats completed the choice traversal session.

#### **3.4 dHPC-Re input is necessary for encoding spatial memories on DNMP task**

Maïsson et al., (2018) showed that Re output was necessary for accurate SWM performance during the sample (memory encoding period) traversal of a DNMP task. Corroborating that study, we first looked at the dHPC-Re pathway by optogenetically suppressing the Re during the individual sample, delay (memory maintenance), or choice (memory retrieval) phases of the DNMP task (Figure 2B). A paired samples t-test revealed the dHPC-ArchT neural suppressor group performed with significantly less choice accuracy during the light-on trials ( $M = 68.333\%$ ,  $SD = 10.866$ ) compared to during light-off trials ( $M = 88.333\%$ ,  $SD = 7.454$ ) on the sample traversal of the DNMP task ( $t(4) = 2.953$ ,  $p = 0.0412$ ). In comparison, the dHPC-tdTomato control group performed with similar accuracy during both the light-on ( $M = 80.556\%$ ,  $SD = 12.546$ ) and light-off ( $M = 83.333\%$ ,  $SD = 5.27$ ) trials on the sample traversal of the DNMP task. These results complemented Maïsson et al., (2018) by describing the Re

as a vital component for encoding spatial information. Specifically, the dHPC-Re projections during the sample phase of a DNMP task were necessary for accurate SWM performance. There were no significant differences in choice accuracy between light-on and light-off trials during the delay period in the dHPC-ArchT neural suppressor group ( $t(3) = 0.6956$ ,  $p = 0.5367$ ). In comparison, there were no significant differences in performance accuracy on the delay phase across the dHPC-tdTomato control group when looking at light-on to light-off trials. Similarly, there were no significant differences in choice accuracy between light-on and light-off trials during the choice traversal of the dHPC-ArchT neural suppressor group ( $t(4) = 1.0681$ ,  $p = 0.3456$ ). And again, there were no significant differences in performance accuracy on the choice phase across the dHPC-tdTomato control group when looking at light-on to light-off trials. Therefore, the dHPC-Re pathway was not necessary for supporting memory maintenance during the delay period or memory retrieval during the choice traversal on the DNMP task. However, since there was an occasional drop in performance accuracy across both control and experimental rats when they went from light-off trials to light-on trials, we decided to examine whether there was an overall effect of turning on the light. According to the original light-by-group 2x2 mixed design ANOVA test (see Statistical Analysis section of Methods chapter), we noted that there was a significant overall effect of light-on trials during the sample traversal across dHPC-injected rats ( $F(1,11) = 7.4741$ ,  $p = 0.0073$ ). This could be the result of the light acting as a visual distraction that seeped out of the fiber stub and reflected off parts of the maze when it turned on. While the effect of light may have bolstered a

significant effect in the ArchT+ group when performing the sample traversal, the ArchT- group experienced the same light and also decreased in performance accuracy during light-on trials as depicted in Figure 2C.

### **3.5 mPFC-Re input is necessary for encoding and retrieving spatial memories on DNMP task**

We then examined the mPFC-Re pathway's task-specific contributions made to accurate SWM performance on a DNMP task (Figure 2C). A paired samples t-test revealed the mPFC-ArchT neural suppressor group performed with significantly less choice accuracy during the light-on trials ( $M = 72.915\%$ ,  $SD = 10.486$ ) as opposed to light-off trials ( $M = 87.501\%$ ,  $SD = 8.334$ ) during the sample traversal of the DNMP task ( $t(3) = 7.0059$ ,  $p = 0.0060$ ). In comparison, the mPFC-tdTomato control group performed with similar accuracy during both the light-on ( $M = 78.333\%$ ,  $SD = 11.18$ ) and light-off ( $M = 83.333\%$ ,  $SD = 10.206$ ) trials during the sample traversal of the DNMP task. These data are consistent with Maisson et al., (2018) by showing that the Re acts as a crucial component for helping to encode spatial information. Essentially, the mPFC-Re projections during the sample phase of a DNMP task were necessary for accurate SWM performance. Optogenetic suppression of the mPFC-Re pathway during the choice traversal was also associated with a decrease in performance accuracy on the DNMP task. A paired samples t-test revealed that perturbing the mPFC-Re projections during the choice traversal light-on trials ( $M = 68.333\%$ ,  $SD = 10.865$ ) caused the rats to perform poorly compared to the choice traversal light-off

trials ( $M = 86.667\%$ ,  $SD = 4.564$ ) on the DNMP task ( $t(4) = 4.4907$ ,  $p = 0.0109$ ). In comparison, the mPFC-tdTomato control group performed with similar accuracy during both the light-on ( $M = 79.167\%$ ,  $SD = 10.758$ ) and light-off ( $M = 85.417\%$ ,  $SD = 4.167$ ) trials on the choice traversal. Therefore, the mPFC-Re projections during the memory retrieval period of a DNMP task were necessary for accurate SWM performance. Finally, mPFC-Re projection suppression caused no significant differences in choice accuracy between light-on and light-off trials during the delay period ( $t(3) = 0.8704$ ,  $p = 0.4481$ ). In comparison, there were no significant differences in performance accuracy on the delay phase across the mPFC-tdTomato control group when looking at light-on to light-off trials. According to the original light-by-group 2x2 mixed design ANOVA test (see Statistical Analysis section of Methods chapter), we noted that there was a significant overall effect of light-on trials during the sample traversal ( $F(1,9) = 8.6367$ ,  $p = 0.0217$ ) in mPFC-injected rats. There was also a significant overall effect of light on the choice traversal ( $F(1,9) = 14.1751$ ,  $p = 0.007$ ) in mPFC-injected rats. These findings imply the likelihood that the light reflections throughout the maze served as a possible confounding distractor. The effect of when the light turned on is represented in Figure 2B, as both the ArchT- and ArchT+ groups during the sample and choice phases decreased in performance accuracy during light-on trials.

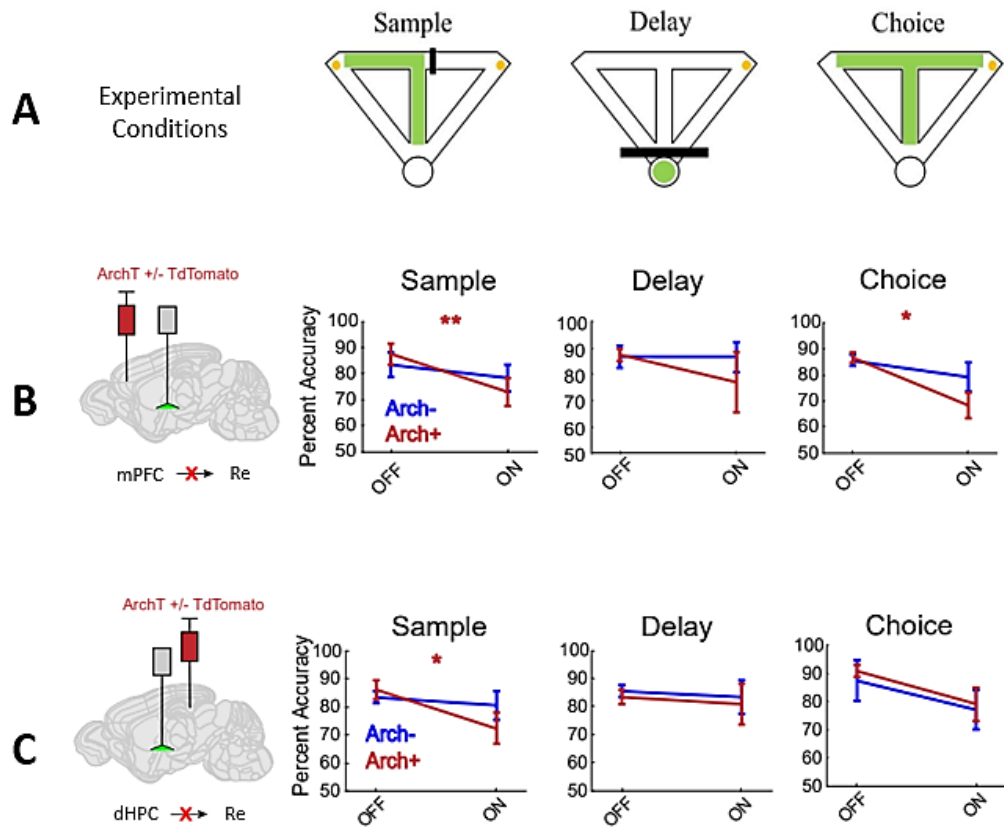


Figure 2: mPFC and dHPC input to Re during different DNMP task phases

A.) Diagram to show task-specific light-on (green shading) periods on the T-maze. In the sample traversal condition, the light turned on when the rat first left the start box and entered the stem. The light turned off after the rat left the reward zone (yellow dots). In the delay period condition, the light turned on when the rat entered the start box after finishing the initial sample (memory encoding) phase of a single trial. The light was on for the entire 20 second delay period, while the rat was contained within the start box by a barricade. The light turned off when the rat entered the stem to complete a choice (memory retrieval) traversal of a single trial. In the choice traversal condition, the light was activated after the rat left the start box and

entered the stem, following the completion of the initial sample traversal of a single trial. The light turned off when the rat left the reward zone of that choice traversal. B.) Choice accuracy of the rats that had their mPFC-Re pathway suppressed via ArchT expression compared to choice accuracy of the rats that received the control tdTomato marker injection in the mPFC-Re pathway (n = 5 mPFC-tdTomato (blue) and n = 4 mPFC-ArchT (red)) during the sample phase (paired samples t-test,  $**p = 0.0060$ ), (n = 5 mPFC-tdTomato and n = 5 mPFC-ArchT) during the delay phase ( $p = 0.4481$ ), and (n = 4 mPFC-tdTomato and n = 5 mPFC-ArchT) during the choice phase ( $*p = 0.0109$ ). C.) Choice accuracy of the rats that had their dHPC-Re pathway suppressed via ArchT expression compared to choice accuracy of the rats that received the control tdTomato marker injection in the dHPC-Re pathway (n = 6 dHPC-tdTomato (blue) and n = 5 dHPC-ArchT (red)) during the sample phase (paired samples t-test,  $*p = 0.0412$ ), (n = 5 dHPC-tdTomato and n = 4 dHPC-ArchT) during the delay phase ( $p = 0.5367$ ), and (n = 4 dHPC-tdTomato and n = 5 dHPC-ArchT) during the choice phase ( $p = 0.3456$ ).

## **Chapter 4**

### **Discussion**

#### **4.1 Significance**

This study shows the importance of the dHPC-Re-mPFC circuit's contributions to SWM. We reported that the dHPC and mPFC projections to the Re during the sample phase of the DNMP task were necessary for SWM accuracy. Similarly, we demonstrated that the mPFC projections to the Re during the choice phase of the DNMP task were also necessary for SWM accuracy. Altogether, these findings supported the notion that the dHPC-Re and mPFC-Re pathways are essential for encoding spatial information. These findings additionally revealed that the mPFC-Re pathway is needed for retrieving spatial memories.

#### **4.2 Functional role of anatomical connectivity across the mPFC-Re-HPC circuit**

The Re sends and receives synaptic projections to and from both the mPFC and HPC (Herkenham, 1978; Vertes et al., 2006). Interestingly, some HPC neurons that project to the Re also receive input from the mPFC (Vertes et al, 2007). Furthermore, ventral HPC (vHPC) projections to the mPFC were first described about 30 years ago (Swanson et al., 1981; Ferino et al., 1987; Jay and Witter 1991), however since then, the ventral and dorsal regions of the HPC have been shown to perform different functions (Dong et al., 2009; Marcelin et al., 2012). It is likely that the mPFC and

HPC communicate with each other, with the Re supporting their interactions (Wouterlood et al., 1990; Vertes et al., 2002; Vertes et al., 2006; Vertes et al., 2007; Griffin et al., 2015; Eichenbaum, 2017). Likewise, there are some Re neurons that can project to both the mPFC and HPC (Hoover and Vertes, 2012). Thus, the HPC-Re-mPFC circuit is highly interconnected, and the Re acts as a viable region for orchestrating this interconnectedness as it is anatomically located in the ventral midline area of the brain.

Recently in our lab, we showed that optogenetic suppression of the Re on the sample traversal of the DNMP task reduced rats' SWM accuracy (Maisson et al., 2018), revealing that Re output is essential for encoding spatial information. In the current work, we showed that both the mPFC and dHPC projections to the Re were needed for encoding spatial information during the sample traversal of the DNMP task. Our study additionally showed that mPFC projections to the Re were necessary for retrieving spatial information during the choice traversal of the DNMP task.

The data from this study directly support the notion that input to the Re is essential for encoding task-relevant memories, which then can be stored and utilized for decision making. In a previous study, Hartung et al., (2016) described that the prefrontal cortex (PFC) is needed for supporting theta bursting behavior throughout the midline thalamus. As a result, this PFC-driven bursting helps induce the HPC's distinct activity. In this vein, it is possible that the midline thalamic Re is needed to mediate the interactions between the mPFC and HPC during memory encoding processes. Similarly, in the current study, both the mPFC-Re and dHPC-Re pathways

were shown to be necessary for encoding memories. Therefore, the Re can be acting as a hub for the mPFC and dHPC to communicate during a period of memory encoding, which explains why Maisson et al., (2018) described such clear SWM deficits in rats that had their Re suppressed during the sample traversal of a DNMP task. This study also showed that input to the Re is necessary for retrieving spatial information that can be used for accurate, goal-directed behavior. The mPFC-Re pathway, not the dHPC-Re pathway, is needed for these retrieval processes. This distinct interaction between the mPFC and Re during the choice traversal of a DNMP task may support the notion of directional prefrontal-thalamic communication during a period of memory retrieval.

#### **4.3 Re is implicated in orchestrating mPFC-HPC interactions during select SWM components**

It has been shown through many past studies that mPFC and HPC communication, which partially occurs via synchronized oscillatory local field potentials between the two brain regions, contributes to SWM (Jones and Wilson, 2005; Hyman et al., 2010; O'Neill et al., 2013; Hallock et al., 2016). The mPFC is involved in memory processes and executive functions, such as goal-oriented decision making (Dalley et al., 2004; Sul et al., 2010; De Visser et al., 2011; Hyman et al., 2017). Similarly, the HPC has been shown to act as a vital region for encoding memories and establishing spatial maps within the brain that represent an environment (O'Keefe and Dostrovsky, 1971; O'Keefe and Nadel, 1978; Shapiro and Eichenbaum,

1999). Likewise, SWM on the DNMP task comprises of three core processes: memory encoding, memory maintenance, and memory retrieval. Information about a specific location that was previously visited is required during the memory encoding process (HPC dependent). This information needs to be converted into the working memory and retained over the memory maintenance period (HPC and mPFC dependent). Spatial information is required during the memory retrieval process in order to accurately guide the direction of the subject's behavior during a goal-driven task (mPFC dependent). As a result, the mPFC and HPC interactions with each other are heavily implicated in carrying out a SWM-related task.

Previous data from our lab assessed if the Re orchestrated mPFC-HPC communication (Hallock et al., 2016). This study used muscimol injections to the Re while comparing rats' performance on two tasks, one that required the use of SWM and one that did not. Most importantly, this resulted in decreased HPC-mPFC theta coherence and reduced HPC theta and mPFC gamma cross-frequency coupling. In addition, Re inactivation caused delay period HPC theta that was led by the mPFC and T-junction mPFC gamma that was led by the HPC to deteriorate. Altogether, not only did Re suppression alter the electrophysiological patterns in the HPC and mPFC, but the rats that received muscimol injections to the midline thalamic nucleus also encountered task-performance deficits. Considering this current study, we observed a decrease in choice accuracy when either the mPFC-Re or dHPC-Re pathways were disrupted on the sample traversal of the DNMP task. Therefore, it is probable that the

Re mediates HPC-mPFC oscillatory synchronization and directionality during a period of memory encoding.

The vHPC-mPFC pathway has additionally been implicated in the encoding process associated with accurate SWM performance in rats (Spellman et al., 2015). Utilizing a linear classifier based on mPFC firing rates, goal location of a rat and the distinct task phase (sample phase versus choice phase) was decoded. Nevertheless, Spellman et al. also showed that suppression of the vHPC-mPFC signaling pathway during the sample phase of a DNMP task disrupted location preference but had no effect on task-phase preference. In a different study, it was shown that rat HPC-mPFC theta coherence was elevated during the choice phase of the DNMP task as opposed to the sample phase (O'Neill et al., 2013). Together, these findings imply that preferred directionality between the mPFC and HPC exist and likely depend on whether the animal is encoding or retrieving spatial information. According to our current study, we have described the Re as a vital component for orchestrating the interactions between the dHPC and mPFC during a sample phase, while in the choice phase, the mPFC could have already received direct input from the HPC which it uses to lead the communication via the Re. Thus, direct HPC-mPFC interactions may occur during the sample phase, leaving the mPFC to combine and synchronize both its own input along with HPC input and send the information to the Re during the choice phase. This supports the conclusions drawn by O'Neill et al., (2013), that describe a heightened level of direct synchronization between the mPFC and HPC during the memory retrieval phase of a DNMP task.

#### **4.4 Conclusions**

Ultimately, this study needs more experimental animals across all the groups to accurately describe the effects of perturbing mPFC and dHPC pathways to the Re. Through postmortem histological reports, this study also needs to verify whether 3 of the mPFC-tdTomato and 3 of the dHPC-tdTomato rats received accurate control injections and if those injections successfully projected to the Re. In the future, these types of behavioral studies should implement a way to cover the light seeping out of the optical fiber tip so the effect of light across ArchT- and ArchT+ groups is not present. There is still research that needs to be done in order to understand mPFC-Re-HPC interactions during memory encoding, as well as direct evidence that describes HPC-mPFC theta coherence's relationship with accurate SWM performance. Further studies can expand on the communication that occurs between the mPFC and Re during memory retrieval processes. Moreover, more studies need to explain how the activity of the mPFC-Re-HPC circuit may vary across SWM tasks and task-specific phases due to compensatory mechanisms between pathways. Regardless, this research is the next necessary step for understanding the exact contributions that this circuit makes to memory encoding, memory maintenance, and memory retrieval. This study has important implications for elucidating clinical targets and treatments for patients that experience dysfunctional mPFC-Re-HPC interactions, such as those noted in schizophrenia (Ford et al., 2002; Lawrie et al., 2002; Meyer-Lindenberg et al., 2005; Sigurdsson et al., 2010) and Parkinson's disease (Moustafa and Gluck, 2011).

## REFERENCES

- Aggleton, J. P., Hunt, P. R., & Rawlins, J. N. P. (1986). The effects of hippocampal lesions upon spatial and non-spatial tests of working memory. *Behavioural brain research*, 19(2), 133-146.
- Bolkan, S. S., Stujenske, J. M., Parnaudeau, S., Spellman, T. J., Rauffenbart, C., Abbas, A. I., Harris, A. S., Gordon, J. A., & Kellenbrock, C. (2017). Thalamic projections sustain prefrontal activity during working memory maintenance. *Nature Neuroscience*, 20, 987-996.
- Buzsaki G (2006) *Rhythms of the brain*. New York: OUP
- Claudi, Frederico. "Scientific Drawings." SciDraw, [scidraw.io/?q=brain](http://scidraw.io/?q=brain).
- Colgin, L. L. (2011). Oscillations and hippocampal–prefrontal synchrony. *Current opinion in neurobiology*, 21(3), 467-474.
- Churchwell, J. C., & Kesner, R. P. (2011). Hippocampal-prefrontal dynamics in spatial working memory: interactions and independent parallel processing. *Behavioural brain research*, 225(2), 389-395.
- Czerniawski, J., Yoon, T., & Otto, T. (2009). Dissociating space and trace in dorsal and ventral hippocampus. *Hippocampus*, 19(1), 20-32.

- Dalley, J. W., Cardinal, R. N., & Robbins, T. W. (2004). Prefrontal executive and cognitive functions in rodents: neural and neurochemical substrates. *Neuroscience & Biobehavioral Reviews*, 28(7), 16 771-784.
- De Visser, L., Baars, A., van't Klooster, J., & van den Bos, R. (2011). Transient inactivation of the medial prefrontal cortex affects both anxiety and decision-making in male wistar rats. *Frontiers in neuroscience*, 5, 102.
- Dong, H., Swanson, L. W., Chen, L., Fanselow, M. S., and Toga, A. W. (2009). Genomic-anatomic evidence for distinct functional domains in hippocampal field CA1. *PNAS*, 106, 11794-11799. Eichenbaum, H. (2017). Prefrontal–hippocampal interactions in episodic memory. *Nature Reviews Neuroscience*, 18(9), 547. Ferino, F., Thierry, A. M., & Glowinski, J. (1987). Anatomical and electrophysiological evidence for a direct projection from Ammon's horn to the medial prefrontal cortex in the rat. *Experimental Brain Research*, 65(2), 421-426.
- Ford, J. M., Mathalon, D. H., Whitefield, S., Faustman, W. O., & Roth, W. T. (2002). Reduced communication between frontal and temporal lobes during talking in schizophrenia. *Biological Psychology*, 6, 485-92.
- Franklin, T. B., Russig, H., Weiss, I. C., Gräff, J., Linder, N., Michalon, A., ... & Mansuy, I. M. (2010). Epigenetic transmission of the impact of early stress across generations. *Biological psychiatry*, 68(5), 408-415.

- Griffin, A. L. (2015). Role of the thalamic nucleus reuniens in mediating interactions between the hippocampus and medial prefrontal cortex during spatial working memory. *Frontiers in systems neuroscience*, 9, 29.
- Hallock, H. L., Wang, A., & Griffin, A. L. (2016). Ventral midline thalamus is critical for hippocampal–prefrontal synchrony and spatial working memory. *Journal of Neuroscience*, 36(32), 8372-8389.
- Hartung, H., Brockmann, M. B., Poschel, B., De Feo, V., Hanganu-Opatz, I. L. (2016). Thalamic and entorhinal network activity differently modulates the functional development of prefrontal hippocampal interactions. *The Journal of Neuroscience*, 36(13), 3676-3690.
- Herkenham, M. (1978). The connections of the nucleus reuniens thalami: Evidence for a direct thalamo-hippocampal pathway in the rat. *Journal of Comparative Neurology*, 177(4), 589-609.
- Hoover, W. B., & Vertes, R. P. (2007). Anatomical analysis of afferent projections to the medial prefrontal cortex in the rat. *Brain Structure and Function*, 212(2), 149-179.
- Hoover, W. B., & Vertes, R. P. (2012). Collateral projections from nucleus reuniens of thalamus to hippocampus and medial prefrontal cortex in the rat: a single and double retrograde fluorescent labeling study. *Brain Structure and Function*, 217(2), 191-209.

- Hyman, J. M., Zilli, E. A., Paley, A. M., & Hasselmo, M. E. (2010). Working memory performance correlates with prefrontal-hippocampal theta interactions but not with prefrontal neuron firing rates. *Frontiers in integrative neuroscience*, 4, 2.
- Hyman, J. M., Holroyd, C. B., & Seamans, J. K. (2017). A novel neural prediction error found in anterior cingulate cortex ensembles. *Neuron*, 95(2), 447-456.
- Jadhav, S. P., Rothschild, G., Roumis, D. K., & Frank, L. M. (2016). Coordinated excitation and inhibition of prefrontal ensembles during awake hippocampal sharp-wave ripple events. *Neuron*, 90(1), 113-127.
- Jones, M. W., & Wilson, M. A. (2005). Theta rhythms coordinate hippocampal–prefrontal interactions in a spatial memory task. *PLoS biology*, 3(12), e402.
- Jay, T. M., & Witter, M. P. (1991). Distribution of hippocampal CA1 and subicular efferents in the prefrontal cortex of the rat studied by means of anterograde transport of Phaseolus vulgaris-leucoagglutinin. *Journal of Comparative Neurology*, 313(4), 574-586.
- Lawrie, S. M., Buechel, C., Whalley, H. C., Frith, C. D., Friston, K. J., & Johnstone, E. C. (2002). Reduced frontotemporal functional connectivity in schizophrenia associated with auditory hallucinations. *Biological Psychiatry*, 12, 1008-11.
- Layfield, D. M., Patel, M., Hallock, H., & Griffin, A. L. (2015). Inactivation of the nucleus reuniens/rhomboid causes a delay-dependent impairment of spatial working memory. *Neurobiology of learning and memory*, 125, 163-167.

- Lee, I., & Kesner, R. P. (2003). Differential roles of dorsal hippocampal subregions in spatial working memory with short versus intermediate delay. *Behavioral neuroscience*, 117(5), 1044.
- Marcelin, B., Lugo, J. N., Brewster, A. L., Liu, Z., Lewis, A. S., ...Bernard, C., (2012). Differential dorso-ventral distributions of Kv4.2 and HCN proteins confer distinct integrative properties to hippocampal CA1 pyramidal cell distal dendrites. *The Journal of Biological Chemistry*, 287, 20 17656-17661.
- McKenna, J. T., & Vertes, R. P. (2004). Afferent projections to nucleus reuniens of the thalamus. *Journal of comparative neurology*, 480(2), 115-142.
- Meyer-Lindenberg, A. S., Olsen, R. K., Kohn, P. D., Brown, T., Egan, M. F., Weinberger, D. R., & Bernman, K. F. (2005). Regionally specific disturbance of dorsolateral prefrontal-hippocampal functional connectivity in schizophrenia. *Arch Gen Psychiatry*, 62, 379-86.
- Moustafa, A. A. & Gluck, M. A. (2011). Computational cognitive models of prefrontal-striatal-hippocampal interactions in Parkinson's disease and schizophrenia. *Neural Networks*, 24, 575-591.
- O'Keefe, J., & Dostrovsky, J. (1971). The hippocampus as a spatial map: Preliminary evidence from unit activity in the freely-moving rat. *Brain research*.
- O'Keefe, J., & Nadel, L. (1978). *The hippocampus as a cognitive map*. Oxford: Clarendon Press.
- O'Neill, P. K., Gordon, J. A., & Sigurdsson, T. (2013). Theta oscillations in the medial prefrontal cortex are modulated by spatial working memory and synchronize

- with the hippocampus through its ventral subregion. *Journal of Neuroscience*, 33(35), 14211-14224.
- Paxinos, G., & Watson, C. (2006). *The rat brain in stereotaxic coordinates: hard cover edition*. Access Online via Elsevier.
- Rajasethupathy, P., Sankaran, S., Marshel, J. H., Kim, C. K., Ferenczi, E., Lee, S. Y., ... & Liston, C. (2015). Projections from neocortex mediate top-down control of memory retrieval. *Nature*, 526(7575), 653.
- Shapiro, M. L., & Eichenbaum, H. (1999). Hippocampus as a memory map: synaptic plasticity and memory encoding by hippocampal neurons. *Hippocampus*, 9(4), 365-384.
- Smith, I. T. & Smith, S. L. (2014). Getting it through your thick skull. *Nature Neuroscience*, 17, 1018-1019.
- Sigurdsson, T., Stark, K. L., Karayiorgou, M., Gogos, J. A. & Gordon, J. A. (2010). Impaired hippocampal–prefrontal synchrony in a genetic mouse model of schizophrenia. *Nature*, 464, 763–767.
- Spellman, T., Rigotti, M., Ahmari, S. E., Fusi, S., Gogos, J. A., & Gordon, J. A. (2015). Hippocampal–prefrontal input supports spatial encoding in working memory. *Nature*, 522(7556), 309.
- Sul, J. H., Kim, H., Huh, N., Lee, D., & Jung, M. W. (2010). Distinct roles of rodent orbitofrontal and medial prefrontal cortex in decision making. *Neuron*, 66(3), 449-460.

- Swanson, L. W. (1981). A direct projection from Ammon's horn to prefrontal cortex in the rat. *Brain research*, 217(1), 150-154.
- Vertes, R. P. (2002). Analysis of projections from the medial prefrontal cortex to the thalamus in the rat, with emphasis on nucleus reuniens. *Journal of Comparative Neurology*, 442(2), 163-187.
- Vertes, R. P., Hoover, W. B., Do Valle, A. C., Sherman, A., & Rodriguez, J. J. (2006). Efferent projections of reuniens and rhomboid nuclei of the thalamus in the rat. *Journal of comparative neurology*, 499(5), 768-796.
- Vertes, R. P., Hoover, W. B., Szigeti-Buck, K., & Leranth, C. (2007). Nucleus reuniens of the midline thalamus: link between the medial prefrontal cortex and the hippocampus. *Brain research bulletin*, 71(6), 601-609.
- Viena, T. D., Linley, S. B., & Vertes, R. P. (2018). Inactivation of nucleus reuniens impairs spatial working memory and behavioral flexibility in the rat. *Hippocampus*, 28(4), 297-311.
- Wang, G. W., & Cai, J. X. (2006). Disconnection of the hippocampal–prefrontal cortical circuits impairs spatial working memory performance in rats. *Behavioural brain research*, 175(2), 329-336.
- Weaver, I. C., Cervoni, N., Champagne, F. A., D'Alessio, A. C., Sharma, S., Seckl, J. R., ... & Meaney, M. J. (2004). Epigenetic programming by maternal behavior. *Nature neuroscience*, 7(8), 847.
- Weel, M. J. D.-V. D., Griffin, A. L., Ito, H. T., Shapiro, M. L., Witter, M. P., Vertes, R. P., & Allen, T. A. (2019). The nucleus reuniens of the thalamus sits at the

nexus of a hippocampus and medial prefrontal cortex circuit enabling memory and behavior. *Learning & Memory*, 26(7), 191–205.

Wouterlood, F. G., Saldana, E., & Witter, M. P. (1990). Projection from the nucleus reuniens thalami to the hippocampal region: Light and electron microscopic tracing study in the rat with the anterograde tracer Phaseolus vulgaris-leucoagglutinin. *Journal of Comparative Neurology*, 296(2), 179-203.

Yizhar, O., Fenno, L. E., Davidson, T. J., Mogri, M., & Deisseroth, K. (2011). Optogenetics in neural systems. *Neuron*, 71, 9-34.